Solid Freeform Fabrication 2017: Proceedings of the 28th Annual International Solid Freeform Fabrication Symposium – An Additive Manufacturing Conference
Reviewed Paper

A Mobile 3D Printer for Cooperative 3D Printing

Lucas Galvan Marques, Robert Austin Williams, Wenchao Zhou
The AM³ Lab, Department of Mechanical Engineering, University of Arkansas at Fayetteville
Fayetteville, AR, United States of America; email: zhouw@uark.edu

Cooperative 3D printing is an emerging technology that aims to provide scalability to 3D printing by enabling thousands of printhead-carrying mobile robots to cooperate on a single printing job and to integrate pre-manufactured components during the 3D printing process. At the core of the cooperative 3D printing platform is a mobile robot that can carry different printhead or a gripper. In this paper, we present a mobile 3D printer with a filament extrusion printhead that can be controlled over the Internet. First, we designed a compact mobile 3D printer with an extrusion printhead and four omnidirectional wheels. A wireless communication interface is also developed to send commands to and receive information from the mobile 3D printer. Successful prints have been demonstrated with two developed mobile 3D printers printing cooperatively, which shows the promise of cooperative 3D printing.

1. Introduction

Ever since the invention of stereolithography (SLA) over three decades ago [1], additive manufacturing (AM) has experienced rapid growth from a rapid prototyping tool [2] to a serious contender for digital manufacturing [3]. The industry has been making great leaps on solving the three major issues that stand in the way to an era of digital manufacturing: printing quality, printing speed, and printing capability. To improve the printing quality, extensive research has been performed to understand the physics of various 3D printing processes [4-7] and to optimize the process parameters [8-10]. To increase the printing speed, numerous new 3D printing processes have been developed, such as continuous liquid interface production (CLIP) [11], Project Escher by Autodesk [12], multi-beam laser additive manufacturing (MB-LAM) [13], selective mask sintering (SMS) [14], high-speed sintering (HSS) [15], selective inhibition sintering (SIS) [16, 17], and binder jetting [18]. To enhance the printing capability, various functional materials have been successfully printed, ranging from metals [19], exotic polymers [20], ceramics [21], biomaterials [22], to multiple materials [23, 24].

However, each of the new technologies comes with their own limitations and it remains a challenge to find a solution that can solve all the three major issues at the same time. One critical insight for this challenge is that most of the 3D printers "live in a box", which creates isolation between different technologies and makes it difficult to combine the advantages of different technologies to overcome the limitations of individual processes. Therefore, a solution demands us to think outside the "box". Cooperative 3D printing is an emerging technology that aims to get rid of the "box" by putting the printhead on a mobile platform such that a swarm of mobile robots carrying different printheads can cooperate with each other on a single printing job. The benefits are multifold: 1. the size of the print is no longer limited by the "box" of the 3D printer; 2. it breaks down the barrier for many printheads to work together to improve printing speed; 3. it allows embedding of pre-

manufactured components during the 3D printing process using a mobile robot carrying a gripper to improve printing capability; 4. it enables different 3D printing processes (e.g., Fused Deposition Modeling (FDM), inkjet, automated fiber placement, etc.) to work together to overcome the limitations of individual processes; 5. the printing and the post-processing can both be automated with various mobile robots to enable autonomous digital additive manufacturing (ADAM).

In this paper, as the first step towards ADAM, we present a mobile FDM 3D printer that can be controlled and monitored over the Internet. In section 2, the design of the mobile printer is presented, including the mobile platform, the filament extruder, the circuits, and the network design for communicating with the mobile printer over the Internet. Tests and results are discussed in section 3. Conclusions are given in section 4.

2. Mobile Printer Design

In the envisioned cooperative 3D printing platform, thousands of mobile 3D printers will work together on a factory floor on their assigned printing tasks. To best realize this vision, a set of requirements need to be satisfied for the design of the mobile printer:

1. Be able to move (XY and rotate) freely and print across an entire factory floor;
2. Has compact dimensions to minimize geometric interference with other mobile robots;
3. Has a positioning accuracy of less than 100 um to be comparable with regular FDM 3D printers;
4. Should be able to print plastic filaments like regular FDM 3D printers;
5. Can carry ~ 1kg of printing material;
6. Should have a modualized design such that the printhead can be easily changed with other types of printheads (e.g., a gripper);
7. Be able to perceive its environment through live video camera and sensors;
8. Can communicate and interact with the user over the Internet;
9. Doesn't rely on battery power such that printing is not interrupted by the need for charging;
10. Low-cost and within a budget of ~$1000.

A concept model of the mobile print is designed based on the requirements as shown in Figure 1. The mobile printer consists of four components: a mobile platform, a Z-stage, the main circuit, and the wireless communication system. It moves in the XY plane using omnidirectional wheels and the printhead moves up and down along the Z stage as it prints. The mobile printer connects to the Internet over a Wi-Fi network to send information to and receive commands from a user interface (UI) through a web browser.

2.1 Mobile Platform

The mobile platform is the most critical component of the mobile 3D printer. It replaces the XY stage in a regular 3D printer with a set of omnidirectional wheels to move the printhead in XY direction.

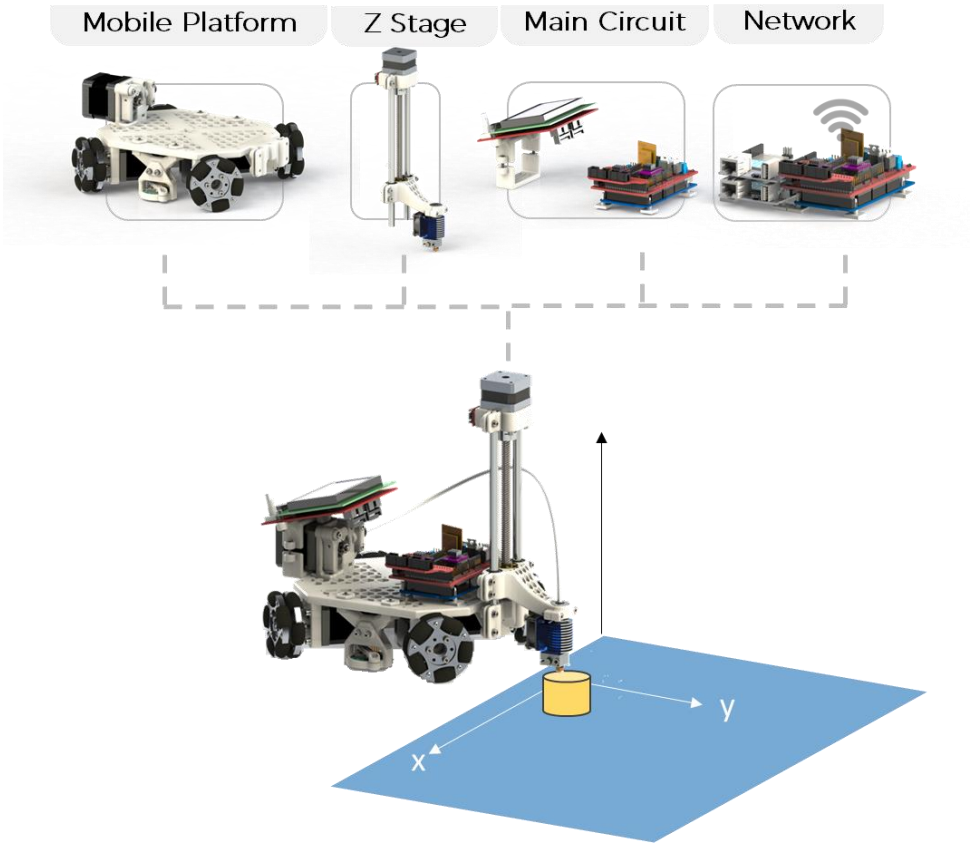

Figure 1. Concept model of a mobile 3D printer with a filament extrusion printhead, which is consisted of four components: (a) the mobile platform; (b) the Z stage; (c) the main circuit; (d) the network system

2.1.1 Initial Design

Many different options exist for omnidirectional wheels, such as 3-wheel or 4-wheel platforms as shown in Figure 2. There are a few considerations in choosing an appropriate omnidirectional wheel platform:

1) Mobility: the movement must resemble the movement of a regular XY stage to simplify the control and the printer design.
2) Load: the platform must be sufficiently powerful to carry the weight of the whole printer and at least 1 kg of printing materials.

Figure 2. Different options for omnidirectional mobile platform

Both 4-wheel platforms satisfy our requirements and we chose the mecanum wheels for

our first design, as shown in Figure 3(a). The first prototype was implemented with four 60-mm mecanum wheels, four NEMA 14 stepper motors with a holding torque of 14 N*cm, and an aluminum body with dimensions of 6 inch by 7 inch.

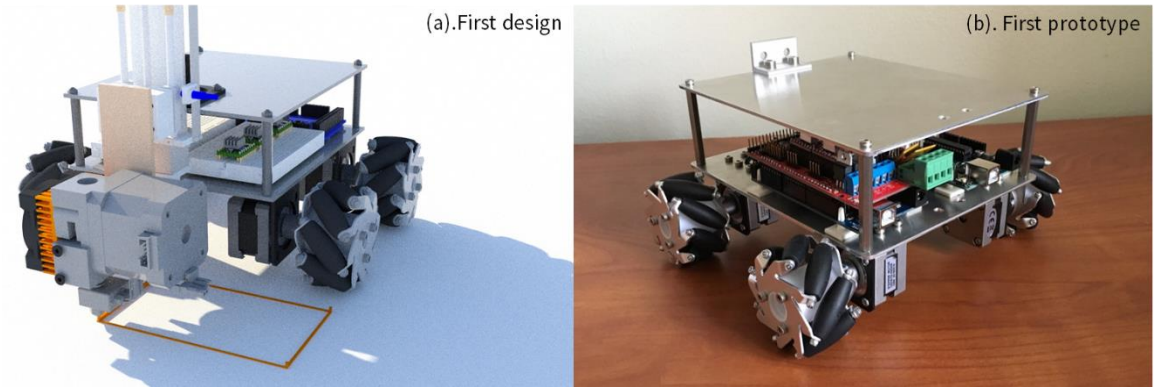

Figure 3. (a): first design; (b): first prototype of the mobile platform

2.1.2 Analysis of Stepper Torque and Wheel Traction

One of the requirements for the mobile printer is that it needs to be able to carry at least 1 kg of printing materials, which will be driven by the stepper motors. Therefore, it is critical to determine if the stepper motors can provide sufficient torque. Assuming the weight of the mobile printer is well balanced among the four wheels, the required torque for each stepper motor can be estimated as:

$$T = F * r \tag{1}$$

where r is the radius of the wheel and F is the friction between the wheel and the floor:

$$F = \mu(m/4)g \tag{2}$$

where μ is the coefficient of friction, m is the total mass of the mobile printer (including the printing material), and g is gravity.

The total mass of the printer (taking into account of 1 kg of printing material) of this design is approximately 3 kg, the radius of the mecanum wheel is 30 mm, and the coefficient of friction of the mecanum wheel on the ground ranges from 0.6 to 0.8. From equation (1), we can estimate the required torque for the stepper motor needs to be larger than 18 N*cm.

The moving speed of the robot U can be related to the rotational speed of the stepper motor ω (rpm) by:

$$\omega = 60 * U/(2\pi r) \tag{3}$$

The maximum printing speed of the mobile 3D printers is designed to match that of a regular FDM 3D printer at 300 mm/s. Therefore, we can estimate the maximum motor speed needs to be larger than 96 rpm. Since the holding torque of the selected NEMA 14 stepper motor is only 14 N*cm, and the running torque at ~100 rpm is usually ~50% of the holding torque, we replace the stepper motor with a high torque stepper (14HS20-1504S)

that has a holding torque of 40 N*cm.

This high torque stepper will be able to drive and the stop the motor in the range of the targeted printing speed. One additional concern is that even though the stepper can stop the rotation of the wheels, the wheels may still slip on the floor. This leads to inaccurate positioning if the inertia of robot is too high:

$$ma > \mu mg \tag{4}$$

where a is the acceleration of the robot. It can be estimated from equation (4) that if the acceleration of the robot is kept below μg (~6 m/s^2), slipping will not happen. There are three possible solutions to this potential issue: 1). limit the max acceleration of the robot in the firmware for path planning; 2). increase the coefficient of friction between the wheels and the floor; 3). use feedback control to compensate.

2.1.3 Positioning

Although we predict slipping will not be a significant issue if we cap the maximum acceleration of the robot, it still happens occasionally due to imperfect contact between the wheels and the floor and imperfect alignment of the wheels, which leads to degradation of printing accuracy over time as shown in Figure 4.

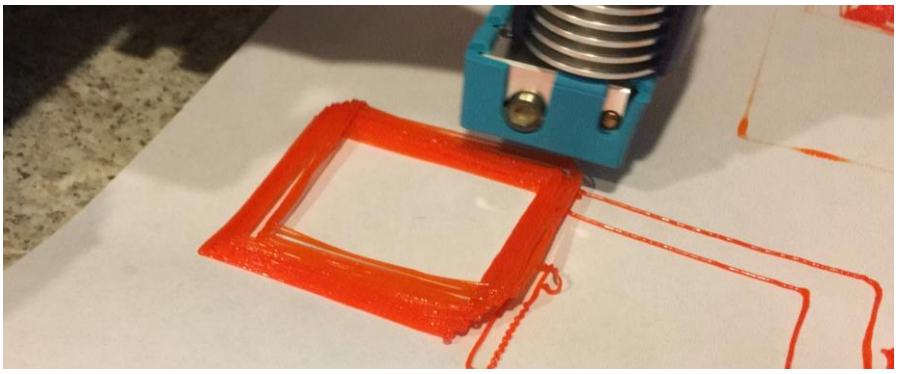

Figure 4. Degradation of printing accuracy over time: the printer is printing a square repetitively.

Therefore, a feedback control system is deemed necessary for the positioning. To choose an appropriate position sensor, a few requirements need to be satisfied:

1. Mobility: the sensor can be carried by a mobile robot and provide location information relative to the ground;
2. Resolution: the sensor needs to have sufficient resolution for the targeted accuracy (~100 um).
3. Sampling frequency: we need to be able to query the sensor at a sufficiently high frequency so that the robot can correct its position in real time.
4. Response time: the sensor can be read in relatively short time and doesn't significantly interfere with the operation of the stepper motors.
5. Speed and acceleration: the sensor needs to be able to provide correct movement information at the max printing speed and acceleration.
6. Cost: the sensor cannot be costly to keep the total cost of the mobile printer below

$1000.

Among various position sensors, an optical mouse sensor satisfies our requirements. It takes a series of pictures at very fast rate and determine the relative movement by comparing the pictures using an optical flow algorithm. We compared two different mouse sensors: one regular PS/2 mouse sensor and the other a laser mouse sensor. The specifications are compared in Figure 5(a). We tested the positioning accuracy of the two sensors by moving them back and forth and compared the readings from the sensors using a microcontroller with the measurements with accurate calibers. As can be seen in Figure 5(b) and (c), the ADNS-9800 sensor performs better and its positioning accuracy is within 5% in the test.

(a). Specification

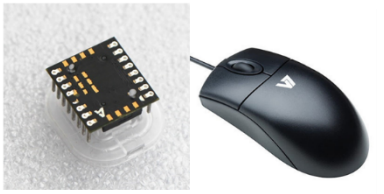

	ADNS-9800	PS/2 Mouse
Resolution	8200 dpi	1000 dpi
Frame Rate	12,000 FPS	3,000 FPS
Speed	150 in/s	28 in/s
Acceleration	30 g	20 g
Lift Detection	Up to 5 mm	Up to 0.75 mm
Communication	SPI	PS/2

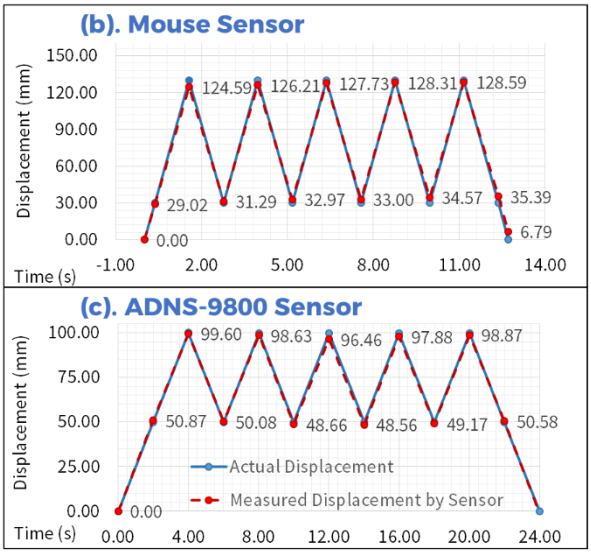

Figure 5. (a) Comparison of important specifications between two sensors; (b) Position accuracy test of the PS/2 mouse sensor by moving the mouse back and forth between 0, 30mm, and 130mm; (c) Position accuracy test of the ADNS-9800 sensor by moving the sensor back and forth between 0, 50 mm, and 100 mm.

In addition to the XY movement, the mobile printer is subjected to one additional degree of freedom (DOF) – rotation about Z axis due to inaccuracy in the wheels. The orientation of the robot must be corrected to perform quality printing over time. One of the solutions is to use an IMU (Inertial Measurement Unit) orientation sensor. We have tested different IMU sensors, including one of the best sensors on the market, the BNO055 9-DOF orientation sensor from Bosch. However, the IMU sensors are not accurate enough to report the correct orientation of the robot due to the small and slow rotation of the robot during printing (the robot usually only rotate a few degrees over 20 minutes). Therefore, we came up with a solution by using two optical mouse sensors as shown in Figure 6. When the robot rotates, the two mouse sensors will report different measurements in Y direction, from which we can derive the rotated angle of the robot based on the distance between the two sensors. The performance of the new solution was evaluated against that of the BNO055 sensor with two tests. In the first test, the robot was rotated back and forth between 0 and 7 degrees and the sensor readings were compared against the actual rotation of the robot as shown in Figure 7(a). It can be seen that the BNO055 sensor performed well in the beginning and gradually drifted off while our solution had excellent performance. In

the second test, a PID control was implemented on the robot so that the robot always returns to 0 degree orientation based on the sensor reading. The robot was then manually thrown off to a random orientation and the readings from the ADNS-9800 sensors and from the BNO055 sensor during this process were compared as shown in Figure 7(b). It is clear that the ADNS-9800 sensors handled the random disturbances very well and always returned the robot to 0 degree while the BNO055 sensor could not.

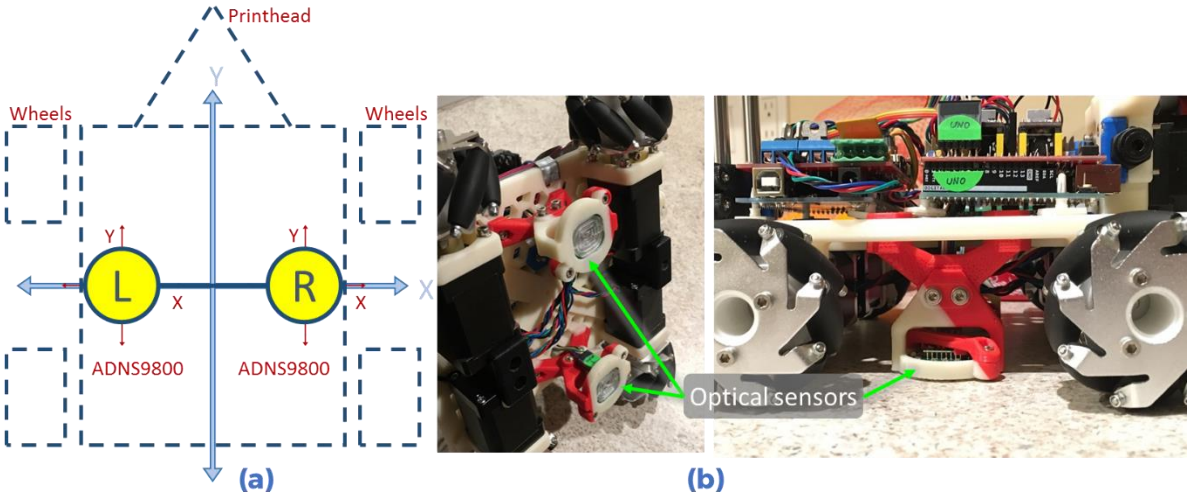

Figure 6. (a) Illustration of how the ADNS-9800 sensors are installed on the robot; (b) the actual installation of the two ADNS-9800 sensors on the robot.

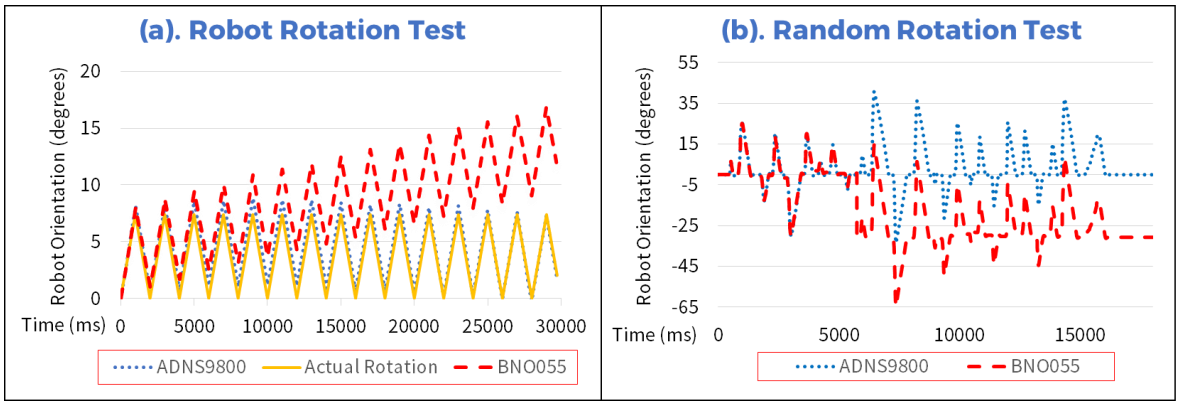

Figure 7. (a) Test 1: the robot was rotated back and forth from 0 to 7 degrees over time and the readings from the ADNS-9800 sensors and from BNO055 sensor were compared with the actual rotation of the robot; (b). Test 2: a PID feedback control is implemented to maintain a zero degree orientation of the robot based on the sensor reading. The robot is then manually rotated to a random angle and the robot tries to return to the zero degree orientation.

2.1.4 Unibody Design

Two additional issues were encountered as we tried to install the Z stage and the extruder on the robot. One was that the weight became imbalanced due to the stepper motor for the extruder as shown in Figure 8. The other issue was that the aluminum body was not strong enough to support the increasing weight of the robot. Increasing the thickness of the aluminum plate will make the robot too heavy. Therefore, we redesigned the mobile platform with a unibody as shown in Figure 9 with a few notable changes:

1. Unibody: We replaced the aluminum plates with a 3D printable unibody to reduce the number of components. The unibody uses a honeycomb structure to maximize the strength to weight ratio and also provides mounting holes for other components.
2. Position sensors: two ADNS-9800 sensors were installed under the unibody to track the location and orientation of the robot.
3. Bowden extruder: the extruder stepper motor was moved to the back of the robot to balance the weight of the robot.
4. Omniwheels: we replaced the mecanum wheels with the omniwheels to increase the traction of the wheels due to its larger coefficient of friction on the same surface.

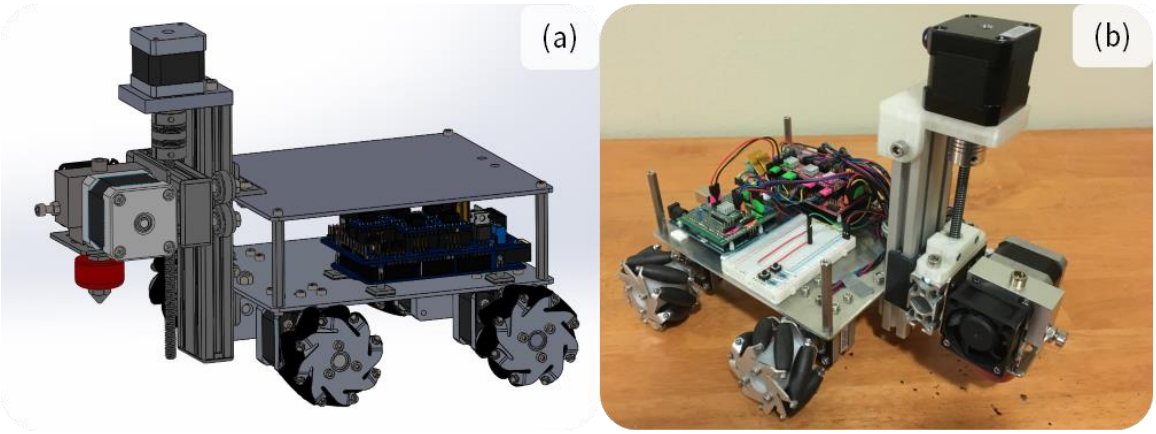

Figure 8. (a) An imbalanced design of the robot; (b) An imbalanced prototype of the robot

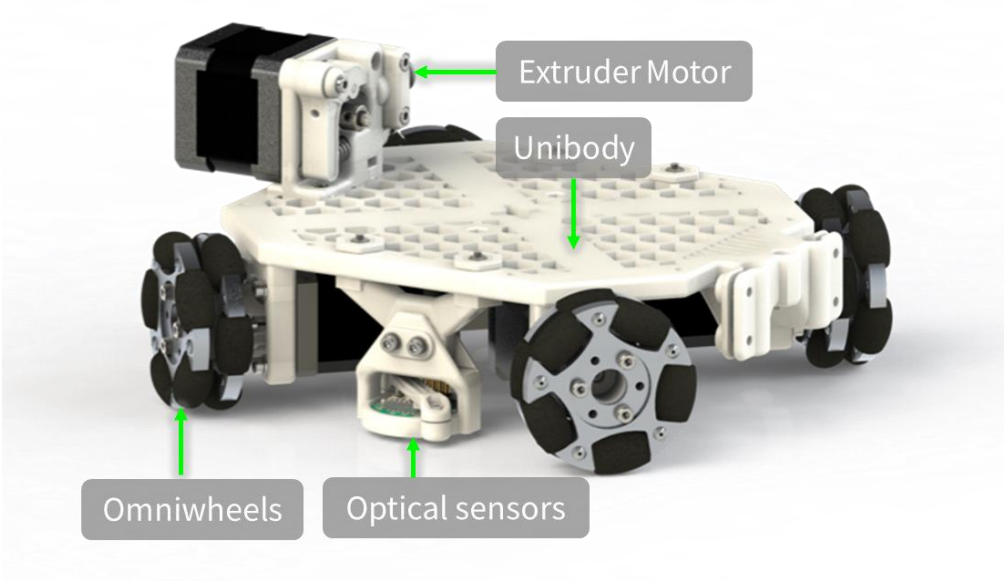

Figure 9. Unibody design of the mobile platform

2.2. Z-stage

Similar to the Z-stage of a regular 3D printer, the Z-stage is responsible for moving the printhead accurately up and down and extrude filaments in coordination with the XY movement based on the input G-code instructions. An exploded view and an assembly of the Z stage are shown in Figure 10. The numbered components are described below:

1. A NEMA 14 stepper motor with a torque of 14 N*cm draws a current of 0.4 A at 12 V.
2. An endstop that is used as a reference point for the Z position of the printhead.
3. A twin-shaft linear guide to guide the linear motion of the printhead in Z direction using two linear shafts (8x200mm). A leadscrew drive in the middle is used to drive the printhead up and down.
4. The two linear bearings provide free motion in the Z axis direction for the print-head.
5. An E3D V6 HotEnd used to extrude ABS, PLA, and other plastics.
6. A 3D printed printhead holder, which can be easily modified to hold different types of printheads (e.g., an inkjet printhead).
7. The T8 nut is attached to the print-head and runs through the threaded rod, making it possible to move the printhead up and down as the rod spins.
8. The Z HOLDER is a 3D printed structure that holds the motor, linear guide, and the end stop switch on top of the Z Stage.

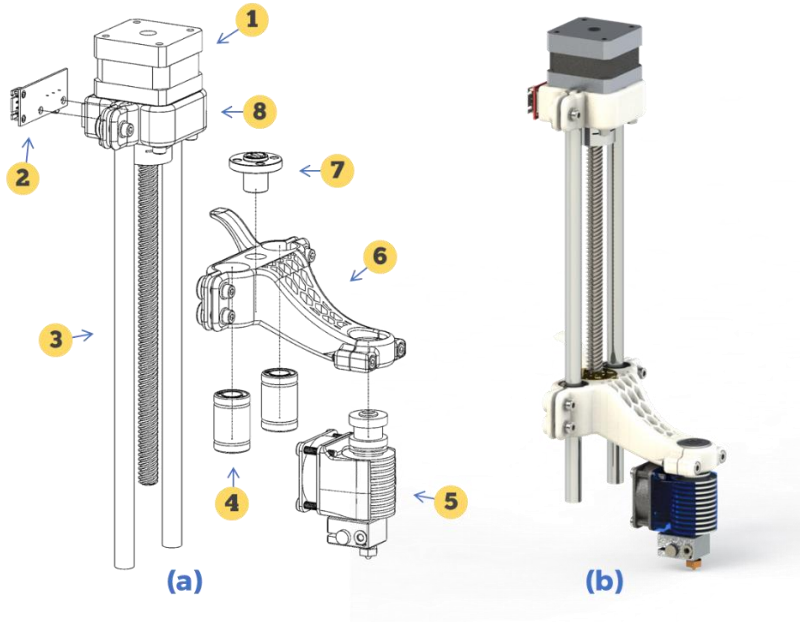

Figure 10. (a) An exploded view of the designed Z stage; (b) An assembled Z stage.

2.3 Main Circuit

The main circuit is similar to a regular 3D printer circuit and controls all basic motion necessary for 3D printing. The main difference is on the XY movement control which is based on wheels instead of linear guides. The main requirements for the circuit design are as below:

1. Translates basic commands (e.g., g-code) into robot movement for printing.
2. Supports at least 6 motors, 1 heater, 1 thermocouple, 6 sensors, 1 fan, and a control panel.
3. Provides sufficient power to drive the mobile printer (e.g., more than 10 A of current at 12 to 24 V).
4. Reads sensor information in ~1ms or less (e.g., SPI communication).

5. Drives all motors simultaneously for coordinated motion (i.e., need to be able to send signals to all motors at the same time for coordinated wheels control).

Based on the requirements, we adapted the circuit of a regular RepRap 3D printer. An Arduino Mega 2560 is used as the central controller of the robot and a RAMPS board is used to control most of the components a regular RepRap 3D printer has, including the motors, temperature sensor, heater, fan, and control panel. A custom board is designed to handle the wheels and the sensors as shown in Figure 11. This board is an extension of the RAMPS board allowing the connection of four extra drivers to control the wheels and a SPI communication hub to connect the optical sensors. The two boards are separated from each other and the connection is made by cables.

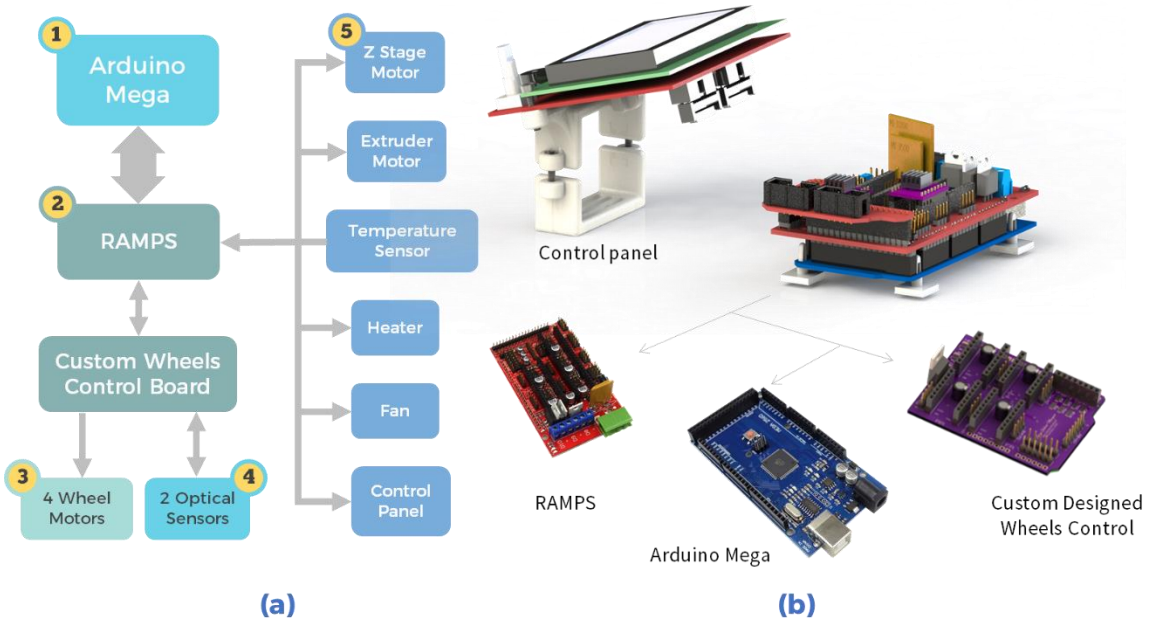

Figure 11. (a) Schematic of the circuit; (b) Prototype of the circuit

2.4. Network Design

To enable cooperative 3D printing, the mobile 3D printers must be able to communicate. To simplify the design of the network for the communication among a swarm of mobile printers, we will connect all individual mobile robots to a central server over a wireless network, which will collect all the information for central planning and coordination. The communication system can be divided into three components:

1. Upstream communication: the mobile robots need to send information to the central server. In this paper, we included three types of information: (a) a live video feed from a camera mounted on the mobile printer; (b) the coordinates of the location of robot; (c) collision warning from collision sensors mounted on the mobile printer.
2. Downstream communication: the mobile robots need to receive commands from the central server. The mobile robot is designed in such a way that it can execute basic commands (i.e., G-code for our robot) to accomplish its basic functionalities (e.g., motion, turn on/off live video, etc.). All the intelligent planning and coordination and other high-level printing strategy will be the responsibility of the

software on the central server, which allows low-cost upgrade of the system (i.e., no need to upgrade each individual robots and the hardware infrastructure but only software on the central server).

3. User interface: although in a complete autonomous setting in the future, human users will not be needed. In the early stage of this technology, it is still necessary to provide the users an interface to operate and interact with the mobile robots remotely.

The upstream and downstream communication are implemented with two Arduino Yun boards with Wi-Fi connection, which are used to handle upstream and downstream communication separately with a web-based user interface (UI) due to the computational intensity for handling video. The Arduino Yun boards communicate with the central controller of the robot (i.e., the Arduino Mega 2560) to gather position and collision information or pass G-code commands as illustrated in Figure 12. The UI provides functionalities for:

- user authentication
- displaying the robot position, collision warning, and live video from the camera carried by the mobile robot
- uploading G-code and AMF files to the robot
- real-time interaction with the robot to move the robot one step at a time
- and previewing the print job with a G-code viewer

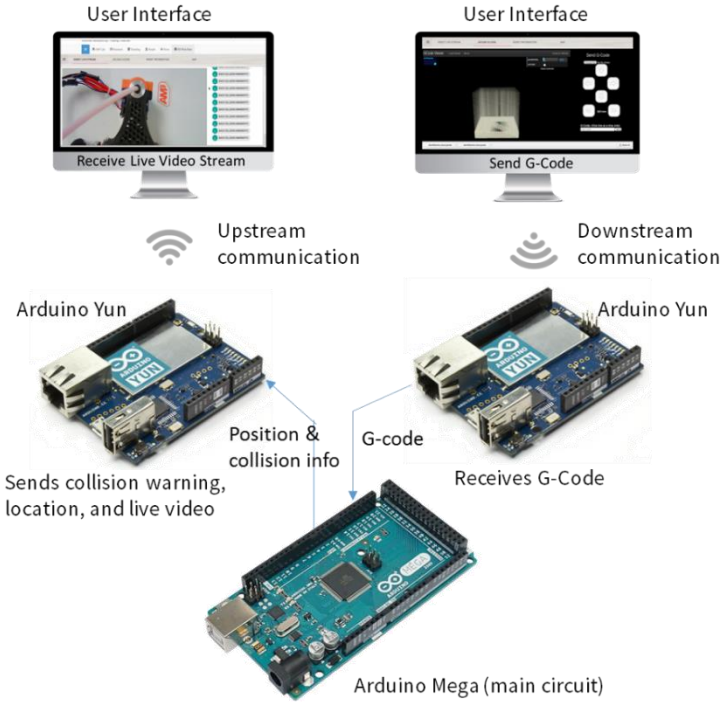

Figure 12. Schematic of the network design of the mobile printer (the two computer screens are from the UI: the left is showing the live video and the collision warning; the right is a G-code viewer to preview the printing job and also provides real-time interaction with the robot by clicking the arrow buttons to move the robot)

3. Testing and Results

After several iterations of redesign and testing, several prototype mobile printers were

developed as shown in Figure 13, in which Figure 13(a) shows a prior design with the Mecanum wheels and Figure 13(b) the prototyped mobile printer with the latest design. The total cost of all the components for each mobile printer is ~$500 with wireless connection (excluding the printed parts, labor cost for manual assembly of the electronics and the robot, etc.). Therefore, it is very feasible to mass produce these robots for under $1000 budget per robot. Because of the low cost of the robots and negligible cost for the infrastructure to support the operation of the robots, it becomes possible to build an economic digital factory in the future equipped with ~1000 of these robots to manufacture a wide variety of products for a few million dollars. We performed two simple tests to demonstrate the functionality of the printer, including the test printing with a single mobile printer and the cooperative printing of two mobile printers.

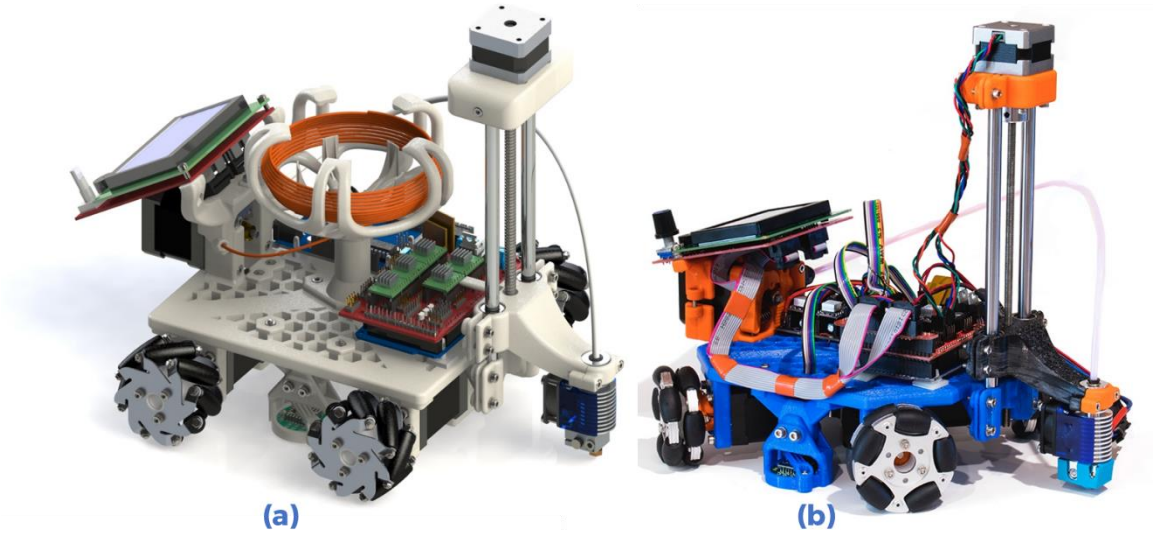

Figure 13. (a) A prior design with Mecanum wheels; (b) A prototype of the latest design with omniwheels (filament spool not included).

3.1 Mobile Printer Test

This test is to demonstrate the mobile printer works. In the test, we designed a CAD model for the letter "AM^3" and used a standard slicer to generate the G-code file. The G-Code file's execution was previewed with a g-code viewer included in the UI. The G-code file was then uploaded to the printer over the Wi-Fi network using the UI.

Snapshots of the printing process is shown in Figure 14. It can be seen the printing was quite successful. The mobile printer first heated the hot end to the temperature specified by the G-code file and then started to extrude and print filaments.

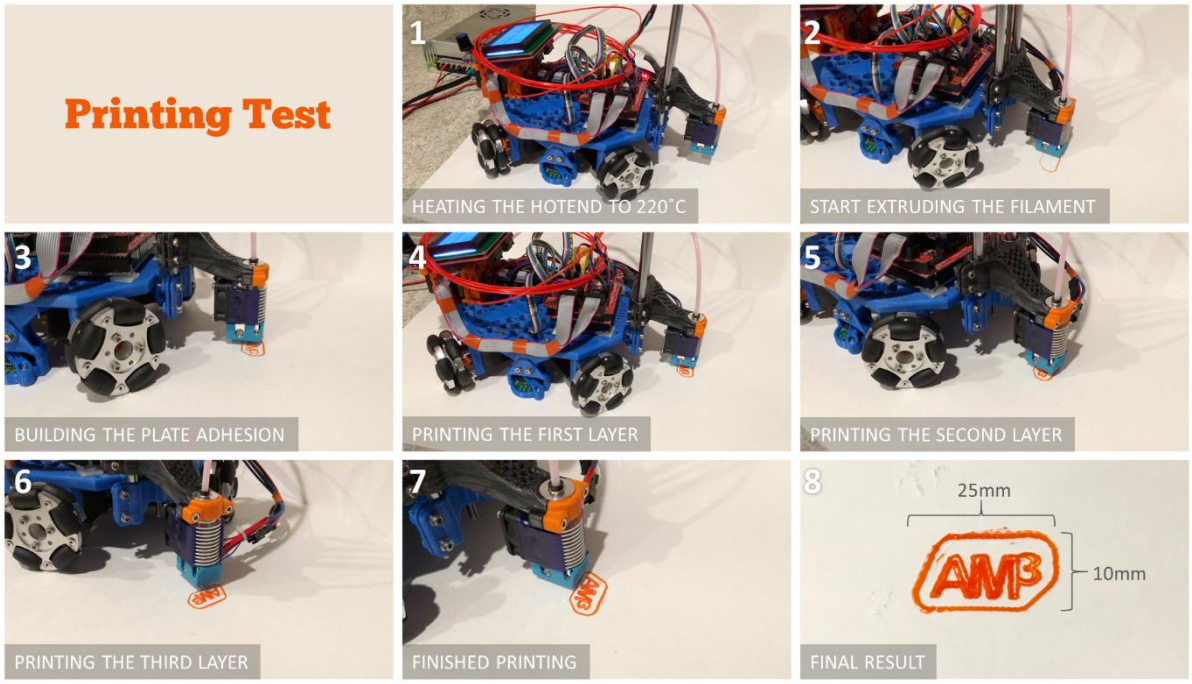

Figure 14. Test of a single mobile 3D printer for printing AM³ using ABS filaments: snapshots at different time of the printing process.

3.2 Cooperative Printing Test

The true potential of this technology lies in its capability for cooperative 3D printing. In this test, we used two mobile 3D printers to accomplish a printing job together, one printing AM³ and the other printing LAB. CAD models of the letters were designed and sliced using a regular slicer and uploaded to the printers wirelessly. Two different color of filaments were used to demonstrate the benefits of cooperative 3D printing, where multi-color, multi-material, or even multi-process printing become possible. The printing was successfully carried out and the snapshots of the printing process are shown in Figure 15.

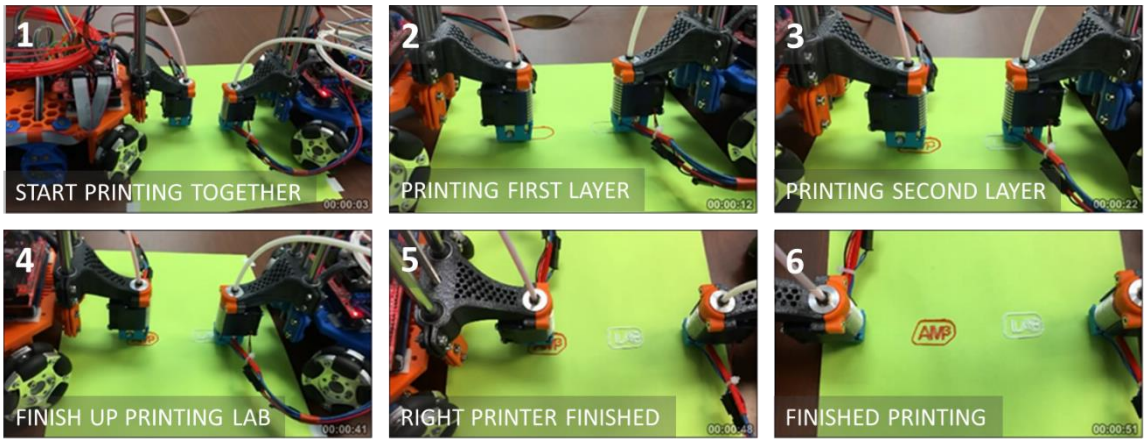

Figure 15. Cooperative printing test: two printers prints together, one printing AM³ and the other printing LAB, with different color of filaments

4. Conclusions

In this paper, we presented a mobile 3D printer for an envisioned cooperative 3D printing platform, where thousands of mobile robots carrying different printheads can work together to print various materials as well as assemble pre-manufactured components autonomously. We first designed a mobile platform and discussed related issues, such as mobility and positioning. A Z-stage with an FDM printhead was then developed to print plastics on the mobile platform. The main control circuit was then developed to enable coordination and control of motion of the wheels and the printing process. Wireless connection was also developed to enable the remote control and monitoring of the mobile printer as well as the cooperation between different mobile printers. Testing results showed that the designed mobile printer worked well. Cooperative printing tests were also performed to demonstrate the potential of cooperative 3D printing as a step towards ADAM as illustrated in Figure 16.

Figure 16. Illustration of ADAM, where a plurality of mobile robots work together autonomously to manufacture complex products with various additive manufacturing processes and digital assembly robots.

5. Acknowledgements

We gratefully acknowledge the financial support from the University of Arkansas, through the startup fund provided by the Vice Provost Office for Research and Economic Development. Any opinions, findings, and conclusions or recommendations expressed in this publication are those of the authors and do not necessarily reflect the views of the University of Arkansas. We also appreciate the participation of undergraduate students during the project, including but not limited to: Kenny Neckles, Jacob Hubbard, and Paolo Vargas.

6. References

1. C. Hull, "*On stereolithography*". Virtual and Physical Prototyping, 2012. 7(3): p. 177-177.
2. J.-P. Kruth, M.-C. Leu, and T. Nakagawa, "*Progress in additive manufacturing and*

rapid prototyping". CIRP Annals-Manufacturing Technology, 1998. 47(2): p. 525-540.
3. S.H. Huang, P. Liu, A. Mokasdar, and L. Hou, "*Additive manufacturing and its societal impact: a literature review"*. The International Journal of Advanced Manufacturing Technology, 2013: p. 1-13.
4. D. Hu and R. Kovacevic, "*Sensing, modeling and control for laser-based additive manufacturing"*. International Journal of Machine Tools and Manufacture, 2003. 43(1): p. 51-60.
5. W. Zhou, "*Lattice Boltzmann simulation of coalescence of multiple droplets on nonideal surfaces"*. Physical Review E, 2015. 92(5): p. 053307.
6. W. Zhou, F.A. List, C.E. Duty, and S.S. Babu, "*Sintering Kinetics of Inkjet-Printed Conductive Silver Lines on Insulating Plastic Substrate"*. Metallurgical and Materials Transactions B, 2015. 46(3): p. 1542-1547.
7. W. Zhou, D. Loney, A.G. Fedorov, F.L. Degertekin, and D.W. Rosen, "*Lattice Boltzmann simulations of multiple-droplet interaction dynamics"*. Physical Review E, 2014. 89(3): p. 033311.
8. F. Lin, W. Sun, and Y. Yan, "*Optimization with minimum process error for layered manufacturing fabrication"*. Rapid Prototyping Journal, 2001. 7(2): p. 73-82.
9. N. Shamsaei, A. Yadollahi, L. Bian, and S.M. Thompson, "*An overview of Direct Laser Deposition for additive manufacturing; Part II: Mechanical behavior, process parameter optimization and control"*. Additive Manufacturing, 2015. 8: p. 12-35.
10. M. Vaezi and C.K. Chua, "*Effects of layer thickness and binder saturation level parameters on 3D printing process"*. The International Journal of Advanced Manufacturing Technology, 2011. 53(1): p. 275-284.
11. J.R. Tumbleston, D. Shirvanyants, N. Ermoshkin, R. Janusziewicz, A.R. Johnson, D. Kelly, K. Chen, R. Pinschmidt, J.P. Rolland, and A. Ermoshkin, "*Continuous liquid interface production of 3D objects"*. Science, 2015. 347(6228): p. 1349-1352.
12. Autodesk. *Project Escher*. 2016 [cited 2017 June 14th].
13. R. Patwa, H. Herfurth, J. Chae, and J. Mazumder. "*Multi-beam laser additive manufacturing"*. in *32nd International Congress on Applications of Lasers and Electro-Optics, ICALEO 2013*. 2013.
14. D.S. Hermann and R. Larson. "*Selective Mask Sintering for Rapid Production of Parts, Implemented by Digital Printing of Optical Toner Masks"*. in *NIP & Digital Fabrication Conference*. 2008. Society for Imaging Science and Technology.
15. H.R. Thomas, N. Hopkinson, and P. Erasenthiran. "*High speed sintering—continuing research into a new rapid manufacturing process"*. in *Proceedings of 17th SFF Symposium, Austin, TX*. 2006.
16. B. Khoshnevis, "*Selective inhibition of bonding of power particles for layered fabrication of 3-D objects"*. 2003, Google Patents.
17. B. Khoshnevis, M. Yoozbashizadeh, and Y. Chen, "*Metallic part fabrication using selective inhibition sintering (SIS)"*. Rapid Prototyping Journal, 2012. 18(2): p. 144-153.
18. J. Moon, J.E. Grau, V. Knezevic, M.J. Cima, and E.M. Sachs, "*Ink-Jet Printing of Binders for Ceramic Components"*. Journal of the American Ceramic Society,

2002. 85(4): p. 755-762.
19. W.E. Frazier, "*Metal additive manufacturing: a review*". Journal of Materials Engineering and Performance, 2014. 23(6): p. 1917-1928.
20. M. Vaezi and S. Yang, "*Extrusion-based additive manufacturing of PEEK for biomedical applications*". Virtual and Physical Prototyping, 2015. 10(3): p. 123-135.
21. N. Travitzky, A. Bonet, B. Dermeik, T. Fey, I. Filbert-Demut, L. Schlier, T. Schlordt, and P. Greil, "*Additive Manufacturing of Ceramic-Based Materials*". Advanced Engineering Materials, 2014. 16(6): p. 729-754.
22. F.P. Melchels, M.A. Domingos, T.J. Klein, J. Malda, P.J. Bartolo, and D.W. Hutmacher, "*Additive manufacturing of tissues and organs*". Progress in Polymer Science, 2012. 37(8): p. 1079-1104.
23. G. Janaki Ram, C. Robinson, Y. Yang, and B. Stucker, "*Use of ultrasonic consolidation for fabrication of multi-material structures*". Rapid Prototyping Journal, 2007. 13(4): p. 226-235.
24. W. Zhou, F.A. List, C.E. Duty, and S.S. Babu, "*Fabrication of conductive paths on a fused deposition modeling substrate using inkjet deposition*". Rapid Prototyping Journal, 2016. 22(1): p. 77-86.